



ENGINEERING SCIENCES

Implications of microbial enhanced oil recovery and waterflooding for geochemical interpretation of recovered oils

LUCIANA G.P. SODRÉ, LAERCIO L. MARTINS, LORRAINE LOUISE G.C. DE ARAUJO,
DANIELLE M.M. FRANCO, BONIEK G. VAZ, WANDERSON ROMÃO, VALÉRIA M.
MERZEL & GEORGIANA F. DA CRUZ

Abstract: Biosurfactants and waterflooding have been widely reported thus far for enhancing oil production. Nevertheless, there is a lack of literature to explore enhanced oil recovered methods effects on its chemical composition. The aim of this work is to investigate the effects of a biosurfactant produced by *Bacillus safensis* and brine injection on the recovered petroleum composition, and their implications for geochemical interpretation. Original and oils recovered from displacement tests were analyzed by gas chromatography and ultra-high-resolution mass spectrometry, emphasizing saturated and aromatic biomarkers and basic and acidic polar compounds. Geochemical parameters based on some saturated compounds were subtly affected by the recovery methods, showing their reliable applicability in geochemical studies. Contrarily, parameters based on some aromatic compounds were more affected by biosurfactant flooding, mostly the low molecular weight compounds. Thus, these aromatic parameters should be applied with caution after such methods. The distribution of basic and acidic polar compounds can also be modified affecting the geochemical interpretation. In the case of the basic ones, the biosurfactant greatly influenced the N class species with favorable loss of lower aromaticity compounds. In addition to water solubilization, the compositional changes described in this study can be related to fractionation due to adsorption on reservoir rocks.

Key words: Biomarkers, biosurfactant, MEOR, oil recovery, petroleomics.

INTRODUCTION

Water injection (waterflooding) and thermal or miscible enhanced oil recovery (EOR) methods are the most worldwide recovery techniques for enhancing oil production (Suleimanov et al. 2020). Further, there are several studies of microbial enhanced oil recovery (MEOR) applications at laboratories and pilot-scale tests (Safdel et al. 2017, She et al. 2019).

The MEOR methods can use biosurfactants, which are amphiphilic molecules, aimed at oil displacement by physicochemical forces. In this case, a chemical interaction occurs among the

injected fluids, the reservoir fluids, and reservoir rocks. Its main mechanism is the decreasing of immiscible fluids interfacial tensions (Kryachko 2018). Despite their benefits, waterflooding and the enhanced oil recovery methods have some misgivings regarding the compositional modification of geochemical analytes by the injected products, which can affect the quality of geological samples and thus compromise their interpretation (Leitenmüller & Rupprecht 2019).

In addition, knowledge of the characteristics of the oil produced is vital to the primary

processing step which has the purpose of separating the gas under controlled operating conditions and removing water, salts, and other impurities making the oil suitable for transfer to the refinery. For refining efficiency, it is essential that know the type of oil that will enter your distillation tower as load, given that fuel quality is obtained by mixing certain hydrocarbons. Furthermore, the analysis of polar compounds is extremely important for the management of refining processes and for determining the economic value of oil (Adiko & Mingasov 2020, Marshall & Rodgers 2004). These uncertainties emphasized the importance of a preview chemical characterization, including non-polar and polar oil compounds produced after any recovery method.

There are few studies in the literature that describe the effects of waterflooding on the properties of the recovered oil. They have proposed that waterflooding may be responsible for removing lighter and water-soluble compounds from the oil, decreasing its API gravity (Li & Zhang 2010, Chang et al. 2016). Following these lines, water washing is the primary cause of composition changes in the water-flooded oil (de Hemptinne et al. 2001). Nonetheless, studies concerning the effects of MEOR method on the produced oil composition, mainly polar fraction, are not reported (Nikolova & Gutierrez 2020). This absence of studies can be related to the difficulty of analysis by conventional analytical techniques since the recovered oils are typically rich in polar compounds (Auflem et al. 2001, Speight 2006). For Hughey et al. (2002), GC-MS simplifies identification by using characteristic patterns of mass fragmentation, in conjunction with retention time, but still suffers from limitations. To overcome that, it is recommended to use high-resolution techniques, however, still little

is used to analyze oils after additional recovery processes.

Gas chromatography with a flame ionization detector (GC-FID) has been applied to assess n-alkanes and isoprenoids in petroleum (Head et al. 2010, Martins et al. 2017). At the same time, GC coupled to mass spectrometry allows the detection of specific saturated biomarkers, such as terpanes and steranes (Peters & Moldowan 1991, Gürgey 1998, Peters et al. 2005) and aromatic compounds (Heckmann et al. 2011). The detection and distribution of these compounds can be applied in geochemical studies regarding oil-oil and oil-source rock correlations, source rock, and oil maturity, organic matter source, and depositional environment, biodegradation, among others (Peters et al. 2005, Larter et al. 2006).

In addition, high-resolution mass spectrometry, such as Fourier Transform Ion Cyclotron Mass Spectrometry (FT-ICR MS), has emerged as an impressive tool that enables petroleum chemical composition analysis at the molecular level, mainly of the heteroatomic polar compounds, such as naphthenic acids and other nitrogen-containing compounds (Rodgers et al. 2005, Oldenburg et al. 2011, Niyonsaba et al. 2019). FT-ICR MS has been also widely applied in geochemical investigations (Hughey et al. 2002, Shi et al. 2010, Vaz et al. 2013, Oldenburg et al. 2014, Poetz et al. 2014, Ziegs et al. 2018). Once each oil compound has a different molecular formula (C_xH_yN_zO_wS_v) with an exact molar mass, it is possible to solve and identify at the same time each one of the thousands of compounds in a complex mixture, with sufficiently high power of mass resolution and precision. Hence, it can separate and select polar oil components depending on their heteroatom class (N_nO_oS_s), number of unsaturation, i.e., double bond equivalent (DBE), and carbon number (CN) (Marshall & Rodgers 2008).

In this context, the purpose of this study is to investigate the potential effects of biosurfactant flooding and waterflooding on the chemical composition of the recovered oils obtained in a previous study (de Araujo et al. 2019), with emphasis on the possible impact on the geochemical interpretation based on saturated and aromatic biomarkers, and mainly basic and acidic polar compounds, once for the latter, there are almost no reports in the literature of their analysis after waterflooding, and as far as known, none after the biosurfactant injection, as proposed here.

MATERIALS AND METHODS

Core flooding experiment and oil samples characterization

The core flooding experiments were performed by oil displacement with 3 wt% NaCl brine. In the MEOR recovery experiment, a 125.0 mg.L⁻¹ biosurfactant solution (equal to 1.3 CMC) was injected at intervals with NaCl brine, as described in more detail by de Araujo et al. 2019. The applied biosurfactant was isolated from the mangrove-derived strain *Bacillus safensis* CCMA-560 based on the procedure previously described by Domingos et al. 2015.

For improving reading comprehension, the crude oil used by de Araujo et al. 2019 is called in the current study as Control Oil, and the oils recovered after the displacement tests as Oil I and Oil II, respectively, to waterflooding and biosurfactant flooding. Control Oil, Oil I, and Oil II were assessed using gas chromatography with flame ionization detector (GC-FID) and by electrospray ionization in positive-ion mode ESI(+) FT-ICR mass spectrometry.

Control Oil, Oil I, and Oil II samples were fractionated on a classical liquid chromatography from which saturated hydrocarbons, aromatics, and polar compounds were obtained using

n-hexane, *n*-hexane:dichloromethane (DCM) (8:2,v/v), and DCM:methanol (MeOH; 9:1,v/v), respectively (details in Martins et al. 2014). The saturated and aromatic fractions were characterized using gas chromatography-mass spectrometry (GC-MS).

Gas chromatography with flame ionization detector (GC-FID)

GC-FID analysis of the total oil samples was performed according to Martins et al. 2017, with an Agilent 6890N GC-FID system with synthetic air, H₂, and N₂ as flame gases, an HP-5 capillary column (30 m x 0.32 mm x 0.25 μm), and 5α-androstane (0.02 mg.mL⁻¹) applied as the internal standard for *n*-alkane quantification. *n*-Alkanes, pristane (Pr), and phytane (Ph) were identified based on the chromatographic profile of reference samples and their retention time.

Gas chromatography-mass spectrometry (GC-MS)

GC-MS analysis of saturated and aromatic fractions was performed in Martins et al. 2017, with an Agilent Technologies 6890N GC with a DB-5 column (30 m x 0.25 mm x 0.25 μm) coupled to an Agilent 5973 MSD mass selective detector. Linear scanning (Scan) analysis in the range of 50-550 Daltons and selective ion monitoring (SIM) were used as the analysis model. The compounds were identified based on literature data, the chromatographic profile of reference samples, and mass spectra.

The saturated biomarkers tricyclic terpanes (TT), 25-norhopane (NH), trisnorneohopane (Ts), trisnorhopane (Tm), regular hopanes (H) and gammacerane (G) were investigated monitoring *m/z* 191, while diasteranes (Dia) and regular steranes (RS) were investigated monitoring *m/z* 217 (Peters & Moldowan 1991). The aromatic biomarkers dimethylnaphthalene (DMN), trimethylnaphthalene (TMN),

phenanthrene (Phe), methylphenanthrene (MPhe), methyl dibenzothiophene (MDBT), and triaromatic steroids (TAS) were investigated monitoring m/z 156, 170, 178, 192, and 198, respectively (Heckmann et al. 2011).

Fourier transform ion cyclotron resonance mass spectrometry (FT-ICR MS)

Oils analyses were carried out in a Solarix 9.4T ESI(+) FT-ICR mass spectrometer and in a 7T Solarix 2xR ESI(-) FT-ICR mass spectrometer (Bruker Daltonics, Bremen, Germany; based on Pinto et al. 2017 and Souza et al. 2018). The chemical profile of the oil sample was analyzed in a positive [ESI(+)] and negative [ESI(-)] modes.

In positive mode, about 1 mg of the oil samples were dissolved in a solution of toluene:methanol (0.67 mg.mL⁻¹), and straightly infused in the ESI sources at a flow rate of 10 μ L.min⁻¹. The instrument was externally calibrated with L-arginine (200-1500 m/z) and settings were: capillary voltage of 3.9 kV; transfer capillary temperature of 220 °C and 2.5 L.min⁻¹ of drying flow. In negative mode, about 1 mg of the oil samples were dissolved in a solution of toluene:methanol (0.5 mg.mL⁻¹), and straightly infused in the ESI sources at a flow rate of 240 μ L.h⁻¹. The instrument was externally calibrated with sodium trifluoroacetate (NaTFA) and settings were: capillary voltage of 4.5 kV; transfer capillary temperature of 200 °C and 4.0 L.min⁻¹ of drying flow.

For ESI(+) mode, a 0.04 s of ion accumulation time was used, with the mass spectra range of m/z 200-1500, accuracy lower than 3 ppm, and resolving power was about 400 000. For ESI(-) mode, a 0.010 s of ion accumulation time was used, with the mass spectra range of m/z 129-2000, accuracy lower than 1 ppm, and resolving power was about 770 000. For both methods, was collected 200 scans.

The mass spectra were internally calibrated with homologous series of neutral [ESI(-)] and basic [ESI(+)] compounds of nitrogen ions (C_cH_hN_n), using the Compass Data Analysis software (Bruker Daltonics, Bremen, Germany), and an algorithm elaborated for petroleum signal processing (Composer software, Sierra Analytics, Pasadena, CA, US) providing the DBE versus CN and Van Krevelen plots. M/z values measurements set the elemental composition of the oil samples, and the class diagrams and DBE distribution were built in Excel spreadsheets.

RESULTS AND DISCUSSION

***n*-Alkanes and isoprenoids by GC-FID**

Figure 1a shows the chromatographic profiles (fingerprint) obtained by GC-FID analyses of the Control Oil, and the recovered oils from the waterflooding (Oil I) and MEOR (Oil II) techniques. It can be observed *n*-alkanes with medium to high molecular weight (*n*-C13 to *n*-C33) in all chromatograms, as well as the high abundance of the isoprenoids pristane (Pr) and phytane (Ph). Furthermore, there is a pronounced hump (UCM - unresolved complex mixture) in the GC chromatograms, which contains compounds not readily resolved by conventional gas chromatography, such as NSO compounds, and compasses many recalcitrant products of biodegradation (Head et al. 2010).

In order to further evaluate the modifications of the hydrocarbon composition in the oil samples after the flooding experiments, it was calculated the total concentration of *n*-alkanes (sum of *n*-C13 to *n*-C33; Fig. 1a) and the concentration of individual *n*-alkanes, in addition to the pristane and phytane (Fig. 1b) for the Control Oil and the recovered oils. Moreover, some parameters used in geochemical studies were determined based on these hydrocarbon compounds, including Pr/*n*-C17, Ph/*n*-C18, Pr/

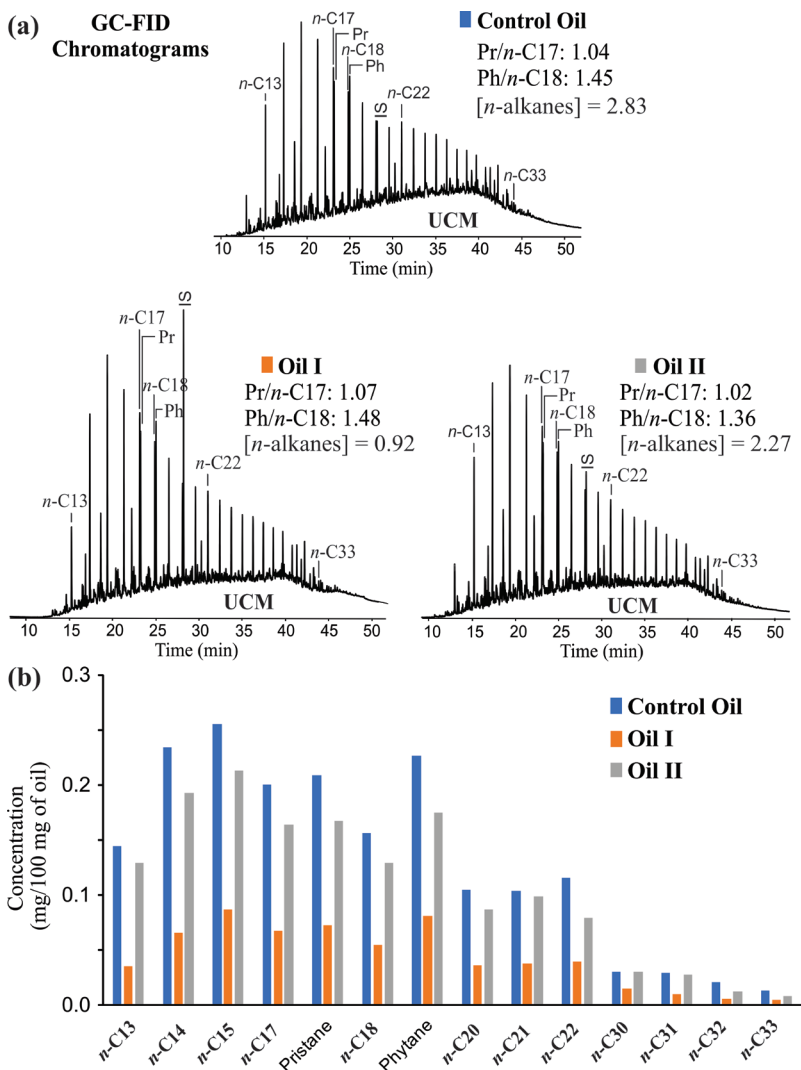


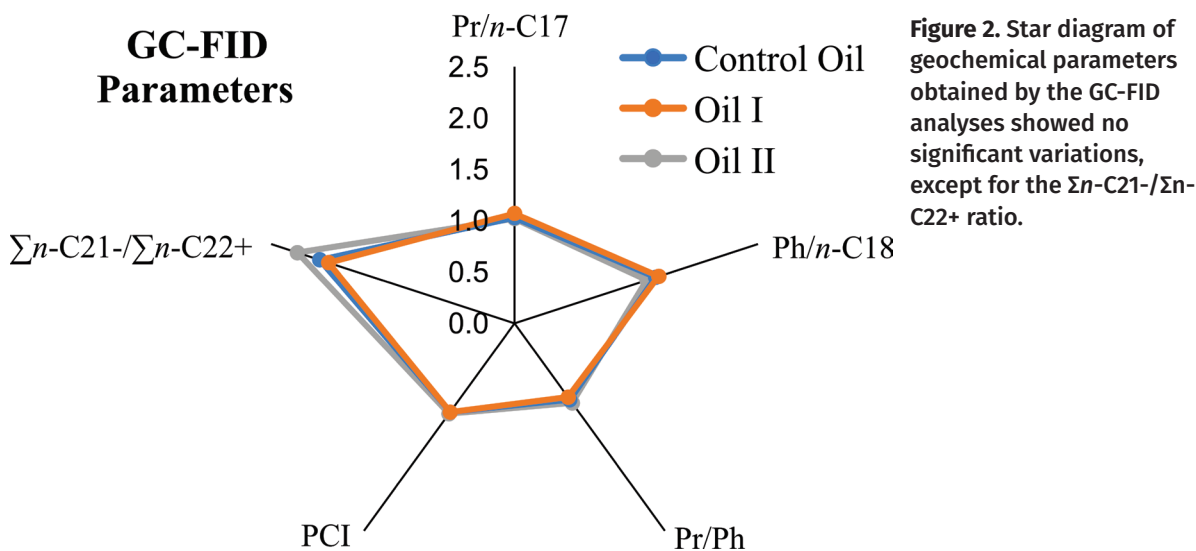
Figure 1. (a) Chromatographic profiles gained by GC-FID analyzes of the three oil samples, presenting the total concentration of *n*-alkanes in mg per 100 mg of oil. (b) The individual concentration of *n*-alkanes and isoprenoids pristane (Pr) and phytane (Ph).

Ph, Σn -C21- / Σn -C22+, PCI (Preferential Carbon Index; Fig. 2; Appendix A - Supplementary Material Table S1).

In contrast to the Control Oil, Oil I and Oil II present a reduction in the total concentration of *n*-alkanes (sum of *n*-C13 to *n*-C33; Fig. 1a), which is expected due to the effects of their adsorption on the rock. Additionally, it is possible to verify that the *n*-alkanes with medium to high molecular mass (*n*-C13 to *n*-C33) and the isoprenoids Pr and Ph were partially removed from the oil sample through both recovery tests, as shown by their lower concentrations to the Oils I and II than the Control Oil (Fig. 1b).

However, it is possible to verify that the individual concentration of these *n*-alkanes and isoprenoids remained greater when using the MEOR recovery method (range of 0.008 to 0.213 mg per 100 mg of oil; Oil II in Fig. 1b), implying a better recovery of saturated hydrocarbons by this enhanced method after the waterflooding. That result suggests that biosurfactants play an important role in mobilizing hydrophobic molecules by reducing their interfacial tension with brine (de Araujo et al. 2019).

The solubility of the lower molecular weight hydrocarbons (*n*-C13 to *n*-C22) in water is more pronounced during the waterflooding process



(Oil I in Fig. 1b) in accordance with Zhu et al. 2003, which presented a reduction in the relative abundance of nonpolar components of low molecular weight and a rise in the abundance of long-chain *n*-alkanes after the primary recovery process. The solubility of these medium molecular weight compounds when using the aqueous solution recovery method can be compared to the water washing process in the reservoir (Li & Zhang 2010, de Hemptinne et al. 2001). Hence, water washing reveals itself as a potential process for changes in oil composition for water injection experiments. The results also agree with a previous study by Bailey & Krouse 1973, which reported that low molecular weight compounds are preferably removed from the oil during contact with water.

Contrary to that observed for *n*-alkanes, especially of low molecular weight, the isoprenoids are less soluble in water (solubility of Pr is 1.0×10^{-8} mg.L⁻¹, and Ph is 1.7×10^{-5} mg.L⁻¹ at 25 °C) and, therefore, the *n*-alkanes are preferably removed on the isoprenoids by water washing. Price 1976 and Xu et al. 2012 observed that the Pr/*n*-C17, Ph/*n*-C18, and Pr/Ph ratios were slightly altered when water was used as a method of oil recovery. However, in the current study, there were no significant changes for

these ratios for Oil I and Oil II compared to the Control Oil (Fig. 2). The preferential carbon index (PCI) also remained relatively constant, resulting in no odd/even carbon preference in both oil recovery processes (Fig. 2). However, the ratio $\Sigma n\text{-C}21\text{-}/\Sigma n\text{-C}22\text{+}$ for Oil II is higher than for Oil I, contrarily the observation in a series of waterflooded wells made by Chang et al. 2016, indicating a later decrease caused by the water washing. Such behavior could be explained if the oil/water interfacial tension is sufficiently high; the biosurfactant could have good interfacial activity for mobilizing the lighter hydrocarbons while the heavier molecular components remain trapped in porous media (Zhu & Lei 2015).

The results on *n*-alkanes and isoprenoids agree with a previous water washing study by Lafargue & Le Thiez 1996, which reported that aliphatic hydrocarbons composition over C15+, including the isoprenoids, shows a little variability. However, aromatic and sulfur-containing compounds varied significantly.

Saturated and aromatic biomarkers by GC-MS

Gas chromatography coupled to mass spectrometry was used since it is a more specific technique than the GC-FID to detect complex molecules such as biomarkers from the terpanes

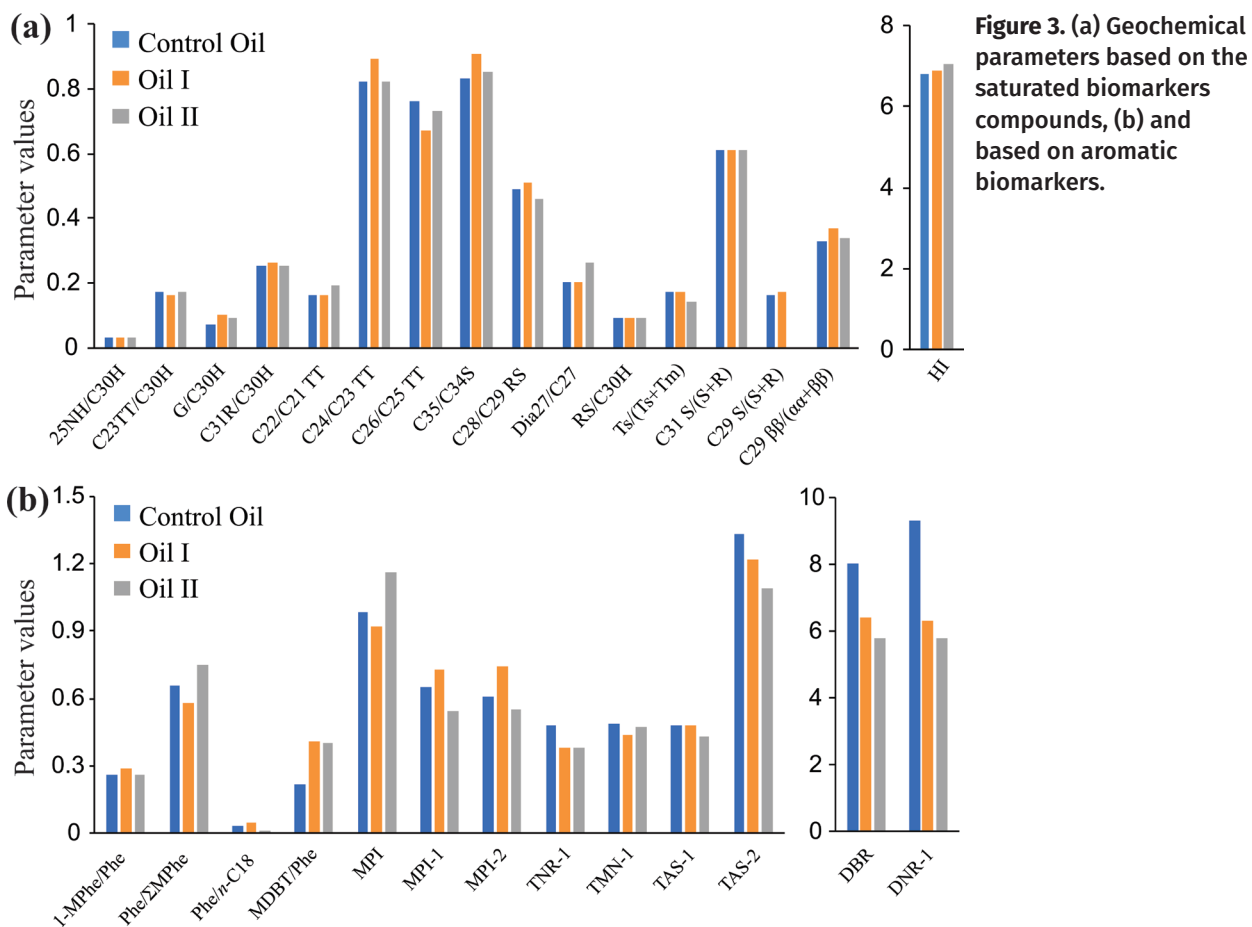
and steranes families (Peters et al. 2005). As shown in Fig. 3a (and Appendix A - Table SII), brine and biosurfactant injections only slightly affected the geochemical parameters based on saturated biomarkers. These parameters encompass essential geochemical proxies (Peters & Moldowan 1991) to distinguish depositional environments of source rocks and to assess oil biodegradation, such as 25NH/C30H, C23TT/C30H, G/C30H, C31R/C30H, C22/C21 TT, C24/C23 TT, C26/C25 TT, C35/C34S, C28/C29 RS, Dia27/C27, RS/C30H, and homohopane index (HI) in addition to parameters for thermal maturity evaluation, such as Ts/(Ts + Tm), C31 S/(S + R), C29 S/(S + R), C29 ββ/(ββ + αα) (Peters & Moldowan 1991).

The ratios C24/C23TT, C28/C29RS, and C35/C34S are more pronounced while the ratio C26/

C25 TT decreased for Oil I. This random behavior is associated with the differences in the low water solubility and adsorption in the rocks for these compounds. Chang et al. 2016 consider that although the values of the C22/C21TT and C24/C23TT ratios are nearly constant, C26/C25TT can decrease in oils recovered with water.

Herein it is also highlighted that the biosurfactant flooding would lead to relatively more constant or slightly affected saturated biomarker ratio values, comparing Oil I and II to the Control Oil. Oil II exhibits an action over the rate Dia27/C27, and additional experiments are required to a plausible explication.

Geochemical parameters based on aromatic biomarkers (Fig. 3b; Appendix A -Table SIII) were more affected by the recovery techniques than the parameters based on *n*-alkanes, isoprenoids,



and saturated biomarkers, in agreement with their higher solubility of aromatic than aliphatic hydrocarbons in water and with previous work (Chang et al. 2018). As observed in Fig. 1a the concentration of *n*-C18 decreased for recovered oils when compared with Control Oil consequently, an increase of the Phe/*n*-C18 ratio was expected, nonetheless, this ratio exhibits an increase in Oil I and decrease in Oil II, indicating an effect of biosurfactant on a lesser recovery of phenanthrene.

The 1-MPhe/Phe ratio is slightly higher in Oil I, and the Phe/ Σ MPhe ratio decrease in the same oil, relative to the Control Oil, which is consistent with the observed by Kuo 1994, that noticed an increase in the methylphenanthrene indices when the oil is recovered with water. The biosurfactant flooding cause an increased in the Phe/ Σ MPhe ratio indicating that methylphenanthenes were less recovered than phenanthrene.

The MDBT/Phe ratio values increased systematically for Oils I and II when compared to Control Oil (Fig. 3b). These results imply a preferred recovery of methyldibenzothiophenes (MDBT) than phenanthrene (Phe) in agreement with the water washing effect since a lower abundance of low molecular mass fractions is reported, in addition to an increase in high molecular mass polycyclic aromatic hydrocarbons (Chang et al. 2016, Zhu et al. 2003).

Nevertheless, the results show a variation in the relative concentration of the methylphenanthenes isomers. The high value of the MPI ratio of Oil II while MPI-1 and MPI-2 values are higher for Oil I, which indicates an increase in 1-MPhe and 9-MPhe. That follows according to Bonilla & Engel 1988, who argue that the relative abundance of 2-MPhe and 3-MPhe decreases with the increase of migration, and consequent adsorption of these minerals from

the rock, which makes the 1-MPhe and 9-MPhe more abundant in the reservoir.

The parameters DBR, DNR-1, and TNR-1 based on dimethyl and trimethylnaphthalene isomers show a substantial reduction after the waterflooding and MEOR. These results point to the influence of adsorption on the distribution of naphthalene isomers during the recovering experiments with brine or aqueous biosurfactant solution, in line with the more solubility of naphthalenes in aqueous solution than phenanthenes (Chang et al. 2016). Furthermore, the decrease in the DNR-1 and TNR-1 ratios for oils recovered with an aqueous solution are consistent with some of the results of Chang et al. 2016, who also verified a reduction in these ratios values after the waterflooding process for two of their samples under study.

Regarding triaromatic steroids, it is possible to verify that the values of the TAS-1 ratio are practically unchanged for Oil I. Indeed, Chang et al. 2016 argues that the parameters based on triaromatic steroids remain relatively constant due to the subtle distinction in water solubility among their isomers. Contrary to that, the values of the TAS-2 ratio showed more considerable variation among the oils, showing a decrease for recovered oils, especially when the biosurfactant was injected. That could be explained by the higher adsorption of C26 TAS 20S by rock compared to C28 TAS 20S, since Trindade & Brassell 1992 report that triaromatic steroids have more significant interaction with rock minerals.

As a result, the parameters based on dimethyl and trimethylnaphthalene, phenanthrene, methylphenanthrene, methyldibenzothiophenes, and triaromatic steroids should be used with caution after brine and biosurfactant injection into the reservoir, specially the DBR and DNR-1 ratio.

Basic polar compounds by ES(+) FT-ICR MS

The oil samples were assessed by ESI(+) FT-ICR MS to investigate changes in the basic polar compounds. The heteroatom class distribution (NnOoSs) of the Control Oil and the recovered oils are shown in Fig. 4a (exhibiting all classes above 1% of the relative abundances). The N class was most abundant in the Control and recovered oils (89, 85, and 59%, respectively), likely encompassing pyridine, quinoline, acridine compounds, and their derivatives (Qian et al. 2001, Terra et al. 2015), followed by the N₂ (4, 3, and 9%, respectively) and NS (7, 5, and 8%, respectively) classes.

Oil I presents a more similar heteroatom class distribution with Control Oil, while Oil II contrasts (Fig. 4). During the core flooding experiments, may occur preferential adsorption and apparent solubility of petroleum components in water (Liu et al. 2004). In this sense, it was possible to notice a slight decrease in the relative abundance of species of N, N₂, and NS classes in Oil I, while Oil II is enriched with compounds of N₂ and NS classes, in addition to the detection of N₄O₄, NO,

NOS, and O₂S classes above 1% likely due to the significant decrease in the relative abundance of the N class. These changes in the composition of the polar compounds after the biosurfactant flooding indicate that the biosurfactant affects the recovery of basic polar compounds from the oil in a particular way.

Regarding the N class, it can be observed in its DBE distribution in Fig. 5a a reduction in the relative abundance in compounds with DBEs between 5 and 14 in the recovered oils in relation to the Control Oil. These compounds slightly decreased in Oil I, whereas Oil II showed more pronounced reductions, with compounds with DBE up to 10 most affected by the MEOR recovery experiments (Oil II). Concerning the N₂ class (Fig. 5b), Oil II also presents the most distinctive profile, showing the higher relative abundance of compounds with DBE between 7 and 25. Although the increased relative lot of N₂ compounds for Oil II should be related to the decreasing in the relative abundance of its N compounds, it is also clear that some reductions are related to low DBE compounds ranging from 7 to 10. The DBE distribution of NS class

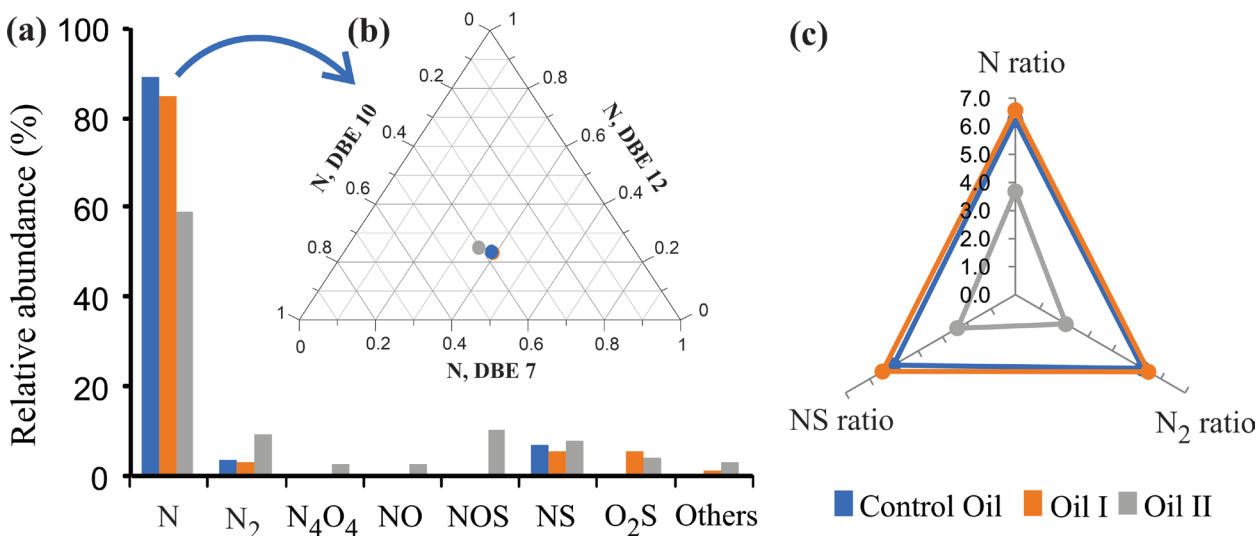


Figure 4. (a) Heteroatom class distributions for Control Oil, Oil I, and Oil II. (b) Ternary diagram used in geochemical studies of maturity assessment illustrating the effect of MEOR (Oil II) on the polar nitrogen compounds of the Control Oil. (c) Star diagram showing the DBE ratios for the N (DBE 4-13/DBE 14-23), N₂ (DBE 8-16/DBE 17-24), and NS (DBE 6-13/DBE 14-21) classes in the Control Oil and the recovered Oils I and II.

for Oil I (Fig. 5c) shows a more similar profile as the Control Oil, although with lower relative abundance. However, the DBE distribution for Oil II shows an increase in aromaticity, with greater relative abundance to compounds with high DBE values (DBE 14 to 21), also presenting the decrease in the relative abundance of lower DBE compounds (mainly with DBE 6 and 7).

The data here suggests there are some intermolecular interactions or side-reactions of N species with the biosurfactant molecule, trapping these complexes in the porous media. The molecular structures of N class species encompassing pyridines, naphthenic pyridines, quinolines, and their derivatives (Terra et al. 2015) could act as nitrogen nucleophile (Solomons et al. 2016) in a reaction with the applied biosurfactant. This biosurfactant belongs to low molecular mass biosurfactants group and it is a surfactin analog, formed by a cyclic lipopeptide composed of a hydroxyl fatty acid chain (de Araujo et al. 2019). Further evidence is needed to confirm this hypothesis.

A ternary diagram (Fig. 4b) usually used to evaluate oil and bitumen maturities (Oldenburg et al. 2014) was plotted, using the relative abundance of the compounds from N class with DBE 7, 10, and 12, being likely quinolines, benzoquinolines, and the most robustness aromatic core structural indenoquinolines or azopyrenes, respectively. This plot is based on that N heteroatom compounds become more aromatic (greater predominance of higher DBE compounds) with increasing thermal maturation (Oldenburg et al. 2014, Poetz et al. 2014). It can be observed in the ternary diagram that there is a more significant alteration in the distribution of compounds in N class in Oil II, which affects the assessment of maturity. Oil II presents a higher abundance of compounds with DBE 10 and 12 and lower DBE 7 than the other oil samples, showing that the lighter and

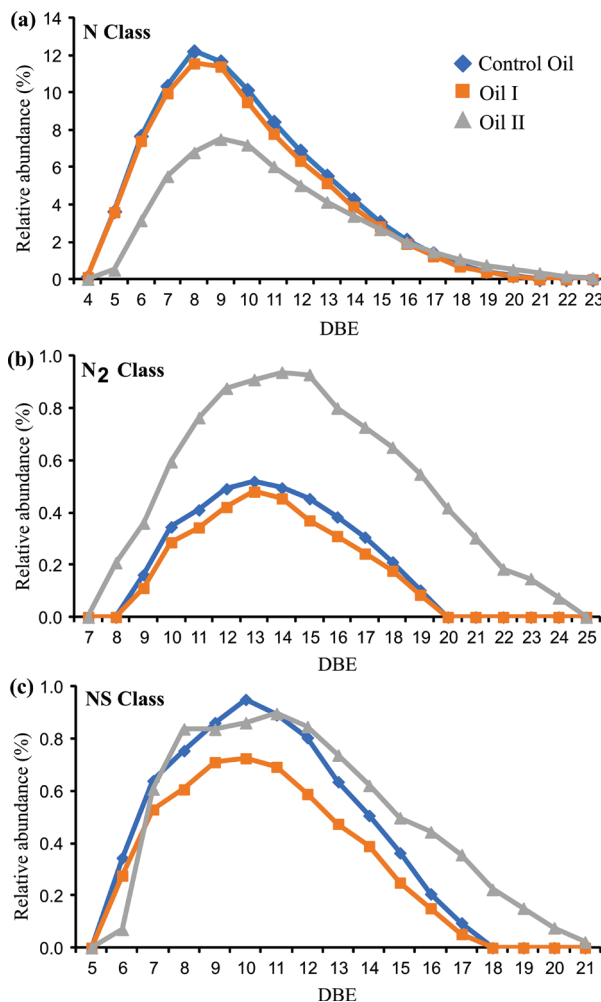


Figure 5. DBE distribution of the N (a), N₂ (b), and NS (c) classes in the Control Oil and the recovered Oils I (from waterflooding) and II (from MEOR).

less aromatic compounds, such as quinolines, were more affected.

To further investigate the decrease in the relative abundance of the low aromaticity polar compounds of the N, N₂, and NS classes (Fig. 4c) the following ratios were determined based on the sum of the relative abundance of compounds with lower DBE over the sum of the relative lot of compounds with higher DBE: DBE 4-13/DBE 14-23 for N class; DBE 8-16/DBE 17-24 for N₂ class; DBE 6-13/DBE 14-21. As can be observed in Fig. 4c, only Oil II shows a significant decrease of the lower DBE compounds, which points to the preferential loss of the lower aromaticity

compounds during the MEOR recovery experiment, possibly by water solubilization or rock adsorption. Oil I is more similar to the Control Oil, concerning the nitrogen abundance (Fig. 4a) and its distribution (Fig. 4c). The N compounds with DBE higher than 15 remained primarily unchanged in all oil samples, being more resistant to the oil recovery processes using aqueous solutions and likely less affected by the effects of geochromatography. Moreover, there is a similarity in the DBE range (4 to 20) for the Control and Oil I. However, Oil II shows a clear, distinct trend concerning the others concerning the amount of unsaturation of the molecule, indicating a broader range for the heteroatom classes (DBE 5 to 24).

The effects on the basic polar compounds due to the application of MEOR are highlighted in the DBE versus CN plots of the N, N₂, and NS classes for Oil II (Appendix A - Fig. S1) (Marshall & Rodgers 2008), which have a distinct profile from the Control Oil, as already observed in Fig. 4c and 5. These results corroborate an increase in the relative abundance of basic polar compounds with higher molecular mass and higher aromaticity for the oil recovered with the aqueous biosurfactant solution. Additionally, Fig. S2 (Appendix A) shows the Van Krevelen type diagrams for N_x (N and N₂) of the Control and recovered oils, using the H/C and N/C ratios (Kim et al. 2003, Corilo et al. 2010). It can be observed the same tendency of Oil II to distinguish from the others, since it presents a subtly altered range of the H/C and N/C ratios, suggesting an increase in the number of heteroatoms of these classes (higher N/C) and more unsaturated compounds (lower H/C). In general, the Control Oil and Oil I show an unsaturation content of 1 to 1.9 and heteroatoms content of 0.015 to 0.08, respectively, with a higher intensity of 1.5 and 0.03. Oil II shows an unsaturation content of 0.8 to 1.9 and heteroatom content of 0.015

to 0.11, with a higher intensity of 1.6 and 0.03, respectively.

Acidic polar compounds by ES(-) FT-ICR MS

The oil samples were assessed also by ESI(-) FT-ICR MS to investigate changes in the acidic polar compounds. The heteroatom class distribution (NnOoSs) of the Control Oil and the recovered oils are shown in Fig. 6a (exhibiting all classes above 1% of the relative abundances). The N class has the highest abundance of all oils, reflecting mainly to the low molecular weight alkylated carbazoles, benzo- and dibenzocarbazoles, with less than three alkyl carbon substituents (Oldenburg et al. 2014). The O class has the second greatest abundance, which encompasses likely components with a hydroxyl functional group able to be deprotonated (Oldenburg et al. 2014), mostly related to phenolic compounds (Shi et al. 2010). The O class occurrence is generally reported in source rocks and crude oils (Vaz et al. 2013, Poetz et al. 2014, Cui et al. 2014, Pereira et al. 2013, Mahlstedt et al. 2016, Oldenburg et al. 2017, Wan et al. 2017, Rocha et al. 2017). The O₂ class is also in high abundance, mainly composed of naphthenic carboxylic acids (Larter et al. 1997, Kim et al. 2005).

According to Fig. 6a Control Oil and Oil II, obtained after MEOR, have more similarities in their heteroatom class distribution, with similar high abundance for the N, O, NO₂, and O₃S classes. However, Oil I show an increase in N and O classes' relative abundances, while there is a decrease in NO₂ and O₃S classes, beyond the suppression of NO₂S and O₃S₂ classes. For cases of nitrogenous compounds reduction in recovered oils (I and II), this suggests that these compounds and their analogs may be preferentially adsorbed by a rock or carried out by the injected solutions (Larter et al. 1997).

The changes in the composition of acidic polar compounds also affect the geochemical

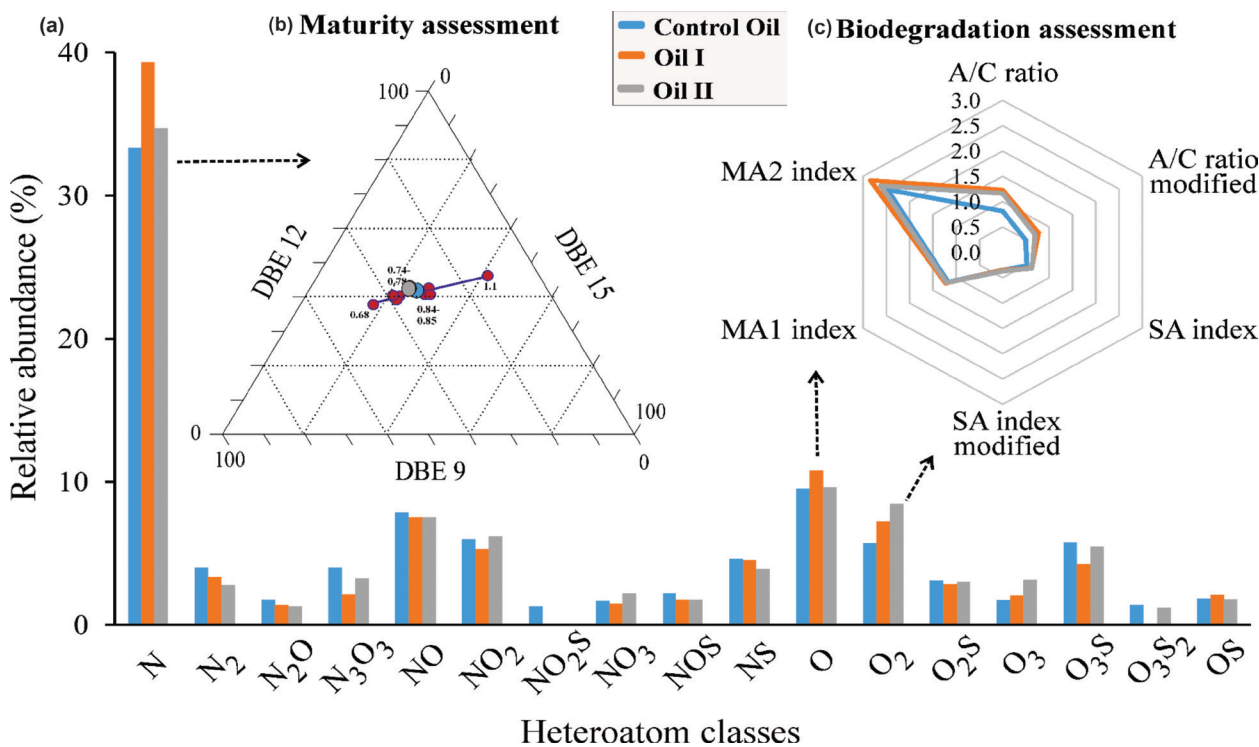


Figure 6. (a) Distribution of heteroatom classes, (b) triangular, and (c) star plots illustrating the maturity and biodegradation assessment, respectively, for the oil samples.

assessment of the recovered oils using the ESI(-) FT-ICR MS data. In this way, Fig. 6b presents a triangular diagram based on the N class distribution commonly used to assess thermal maturity of oils (Oldenburg et al. 2014), using the distribution of carbazoles (DBE 9), benzocarbazoles (DBE 12), and dibenzocarbazoles (DBE 15). It can be seen that all three samples are in the 0.74 and 0.84% vitrinite reflectance equivalent (%Re) range compared with Oldenburg et al. 2014 results, which indicate oils in the oil window. However, there was a subtle change in the maturity assessment of the recovered oils, with both classified with a slightly lower maturity level than the Control oil due to the higher proportion of N-compounds with DBE 9 and 12 than 15. This behavior can also be seen in Fig. 7a showing that there was a significant increase in the relative abundance of N class for oils I and II mainly regarding carbazoles (DBE

9) benzocarbazoles (DBE 12) when compared to Control oil.

Fig. 7b shows the DBE distribution of O class species ranging from 4 to 17, and it is also observed an increase in the relative abundance of low DBE compounds for the recovered oils compared with the Control oil, mainly those with DBE 4, 5, and 6. This is more pronouncedly even in oil I, when compared to Control Oil.

The Fig. 8a-b shows the carbon number distributions for O class compounds with DBE 4 and DBE 5, typically ranges from 13 to 67 (Martins et al. 2021), with greater relative abundance of species with 27 and 28 carbon atoms. These compounds have been commonly reported in studies of crude oils, and rock extracts by ESI(-) FT-ICR MS, and the ones with DBE 5 are mostly methyl- and dimethyl-isoprenoidyl phenols (Zhang et al. 2011, Martins et al. 2021), although some works have interpreted them as sterol-like compounds (Oldenburg et al. 2014, Rocha

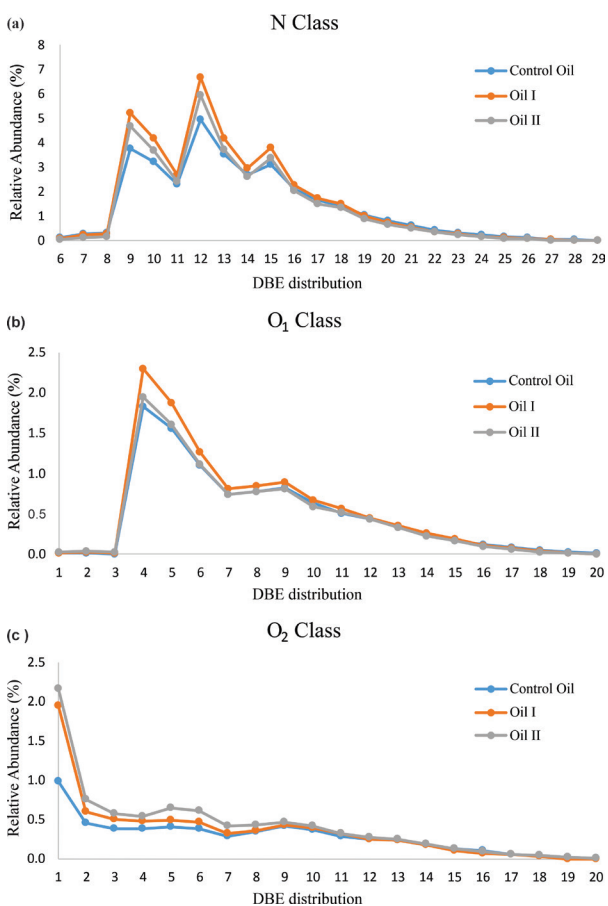


Figure 7. DBE distribution of (a) N, (b) O, and (c) O₂ classes for the oil samples.

et al. 2017). It is then perceived for oils I and II a significant relative decrease in medium to high molecular weight compounds (carbon number 22 to 50) in DBEs 4 and 5 and this occurs mainly in oil recovered with biosurfactant. That could be strongly related to the water washing process that occurs when injecting solutions into the reservoir in order to recover the oils, with the consequent solubilization of these aromatic compounds in the water. It is worth mentioning the water washing may be the dominant process for changes in oil composition in experiments carried out with aqueous solutions (Chang et al. 2016, de Hemptinne et al. 2001).

Regarding the O₂ class (Fig. 7c), the DBE distribution ranges from 1 to 20. It was verified that all the samples have a predominance of

DBE 1 compounds (acyclic acids), which are mostly reported as fatty acids (Rocha et al. 2019, Martins et al. 2021). However, a markedly high relative abundance of DBE 1 compounds was verified in Oils I and II. Fig 8c shows the carbon number distributions for O₂ class compounds with DBE 1, ranging from 12 to 50. Fatty acids (DBE 1) that dominate the O₂ compounds typically range from carbon number 12 to 48 (Martins et al. 2021). By the plot, it is possible to identify a predominance of compounds with carbon number 16 and 18. The abundant O₂ compounds with DBE 1 and 16 carbon atoms likely correspond to hexadecanoic acid (VIII-a; C₁₆H₃₂O₂) (Shi et al. 2010, Liu et al. 2015, Han et al. 2018a). It is noticed once again that oils I and II have a different trend than Control Oil. There is an increase in the relative abundances of low DBE compounds (mainly DBE 1 to 7; Fig. 7c).

The presented changes on the O and O₂ classes also affect the geochemical assessment based on them. A star diagram was plotted (Fig. 6c) using biodegradation ratios calculated based on the DBE distribution of these classes (prioritizing the most abundant above; according to Vaz et al. 2013, Larter et al. 1997, Kim et al. 2005). O Class DBE 4, for example, slightly affected the monoaromatic index 2 (MA2; DBE 4/7; Larter et al. 1997). The biodegradation trends can be observed, in which DBE 4 (monoaromatic core compounds) is the most abundant (case of the oil I) to non-/slightly biodegraded oil samples (Martins et al. 2017). For the O₂ Class, the high abundance of DBE 1 compounds in the recovered oils (oils I and II) affects more significantly the A/C ratio (acyclic/cyclic acids ratio), modified A/C ratio, and more subtly, the SA index. Only the modified SA index does not change since it is not based on DBE 1 compounds. In general, an A/C ratio higher than 1, as presented for oils I and II, corresponds to a non-biodegraded oil (Kim et al. 2005). This follows in agreement with

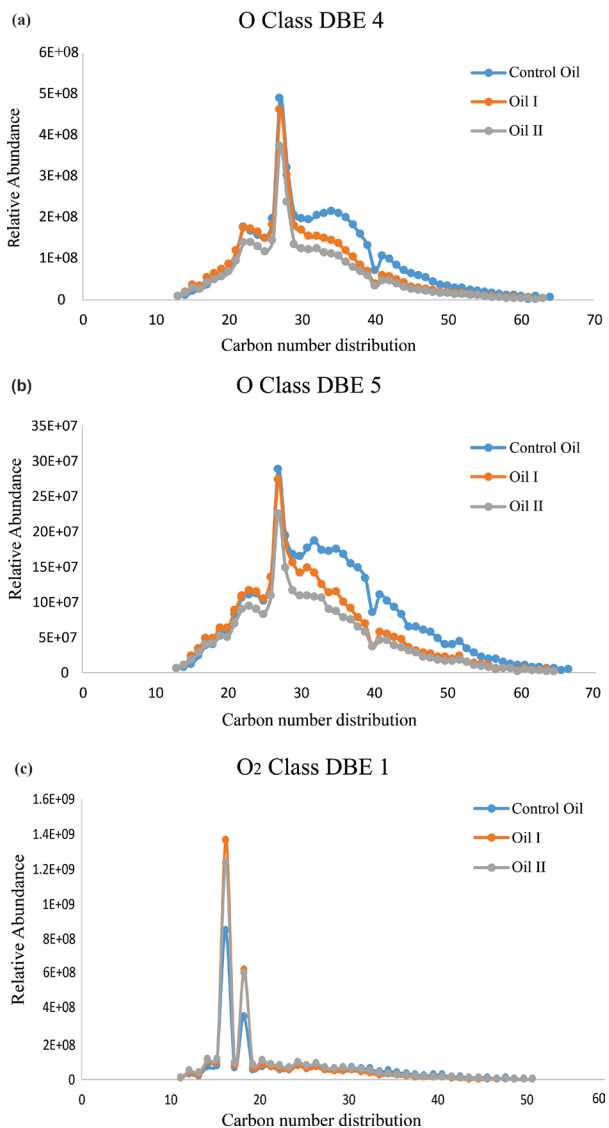


Figure 8. Carbon number distributions of the (a) O Class DBE 4, (b) O Class DBE 5, and (c) O₂ Class DBE 1.

previous studies that applied ESI(-) FT-ICR MS (Hughey et al. 2002, Cui et al. 2014, Mahlstedt et al. 2016, Wan et al. 2017, Rocha et al. 2017), which indicate a predominance of N species in non-biodegraded crude oils (Fig. 6a). However, the Control Oil has an A/C ratio of 0.81, being classified as light to moderately biodegraded oil. Therefore, as with thermal maturity, the applied recovery methods can affect the biodegradation assessment by ESI(-) FT-ICR MS analyses.

In addition, it is already known from previous studies that FT-ICR MS is able to distinguish crude oils from different origins (Hughey et al. 2002, Wan et al. 2017, Rocha et al. 2017). This is possible because both the distribution of heteroatomic compounds and their relative abundance vary according to the geological origins of the oils (Rocha et al. 2017). Thus, to extend the geochemical characterization of the oils, a paleoenvironmental assessment of the three oil samples (I, II, and Control Oil) was carried out, applying the ratios established by Rocha et al. 2018 (Fig. 9), based on the distribution of DBE for the O and O₂ classes, which are among the most abundant classes here. The results indicate changes in the paleoenvironment evaluation among the samples, with oils I and II being classified as a marine while the control oil is classified as lacustrine (Fig. 10). This indicates that the applied recovery methods can affect this geochemical assessment.

Moreover, according to Rocha et al. 2018, the distributions of elementary classes can be used to distinguish lacustrine oils from marine ones. The first significant difference between these two depositional environment conditions

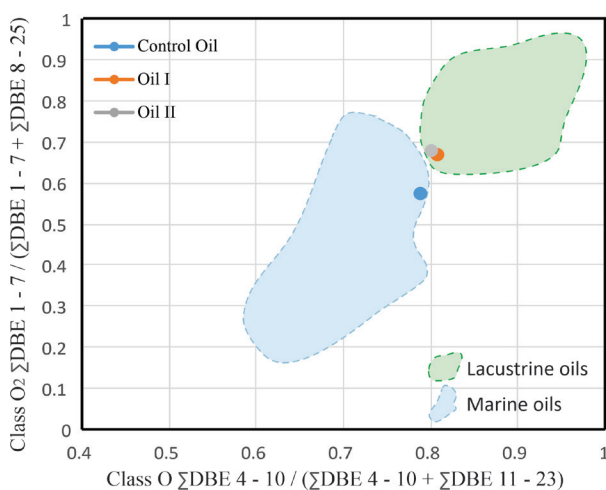


Figure 9. Depositional environment assessment of oil samples (I, II, and Control Oil) based on the distribution of O₁ polar compounds investigated by negative ESI FT-ICR MS.

is related to the Nx and Oz classes, which dominate the fraction of acidic compounds in all samples. Lacustrine oils tend to be enriched with Nx compounds, while marine oils can be distinguished by their more abundance for Oz compounds. The NxOz compounds show a similar distribution in oil samples, regardless of the deposition environments of the generating rocks (Rocha et al. 2018). Thus, the oil samples in the current study were assessed in a ternary diagram (Fig. 10) using the relative amounts of the three major elementary classes: Nx, Oz, and NxOz. The results suggest subtle differences in the distribution of the three oil samples' polar compounds, however, all the samples are more enriched in Nx compounds, indicating lacustrine depositional paleoenvironment of the source rocks of the Control Oil. So, these results demonstrate that the paleoenvironmental assessment by ESI (-) FT-ICR MS analyses can also be affected using the applied recovery methods.

CONCLUSION

Waterflooding and biosurfactant flooding only subtly affect the geochemical parameters based on saturated hydrocarbons. Accordingly, the parameters Pr/*n*-C17, Ph/*n*-C18, Pr/Ph, PCI (preferential carbon index), and Σn -C21-/ Σn -C22+ based on *n*-alkanes and isoprenoids, and several parameters based on tricyclic terpanes, hopanes, gammacerane, diasteranes, and steranes can be reliably applied for geochemical interpretation after brine and biosurfactant injection into the reservoir. In addition, the injection of biosurfactant revealed a more significant recovery of *n*-alkanes and isoprenoids than the waterflooding technique highlighting its potential applicability.

On the other hand, geochemical parameters based on aromatic hydrocarbons

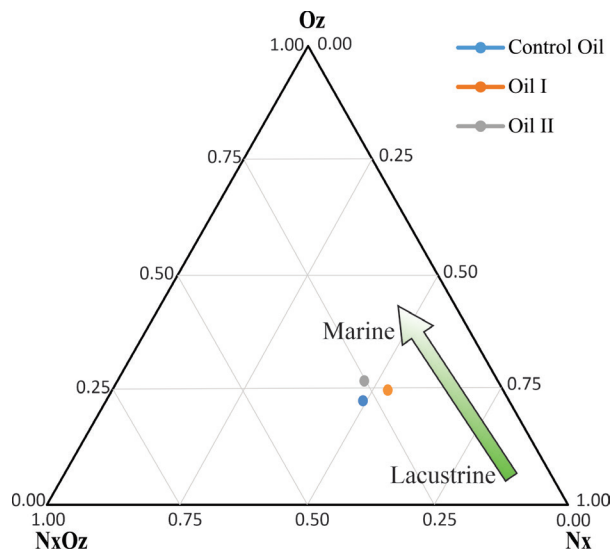


Figure 10. Ternary diagram for the most abundant elemental classes assigned on the negative ESI FTICR-MS results: Nx, Oz, and NxOz, for the oil samples (I, II, and Control Oil).

are affected by biosurfactant flooding and the known effects due to the application of waterflooding. As a result, the parameters based on dimethyl and trimethylnaphthalene, phenanthrene, methylphenanthrene, methyldibenzothiophenes, and triaromatic steroids should be used with caution after brine and biosurfactant injection into the reservoir, especially the DBR and DNR-1 ratios.

The distribution of basic polar compounds can also be modified by the waterflooding and MEOR methods affecting the geochemical interpretation. Nitrogen compounds and their analogs may be preferentially carried out by the injected water, with favorable loss of compounds with lower aromaticity, especially after biosurfactant injection. Likewise, analysis of polar compounds by ESI (-) FT-ICR MS showed that recovery methods can also affect geochemical assessment, such as thermal maturity, biodegradation, and depositional paleoenvironment, based on acidic species, since Oils I and II proved to be different from Control Oil, in general. Further investigation is

still required to comprehensively understand and verify the additional effects of the biosurfactant in the aromatic polar compounds.

So, the study of changes in the chemical composition of petroleum after secondary (waterflooding) and advanced (MEOR) recovery processes, through the analysis of saturated, aromatic, and polar compounds, showed that a chemical investigation of the oils recovered with aqueous solutions is fundamental to properly qualify these oils, since the recovery processes used in this study proved to be able to influence the chemical composition of the oil, especially at the level of geochemical interpretation when the acidic species of the oils were analyzed in depth. Waterflooding is undoubtedly considered one of the most dominant processes for changes in the chemical composition of petroleum, as demonstrated in this work.

Acknowledgments

The authors are grateful to Laísa R. Brasil for the recovered oils from the porous media experiments, and to PETROBRAS for the crude oil donations. This work was performed with financial support provided by Programa de Formação de Recursos Humanos- Agência Nacional do Petróleo (PRH20-ANP), Brazil; by Fundação de Amparo à Pesquisa do Estado do Rio de Janeiro (FAPERJ - Proc. E-26/210.760/2019 and Proc. E-26/210.163/2021), Brazil; and by Coordenação de Aperfeiçoamento de Pessoal de Nível Superior (CAPES - Finance Code 001), Brazil.

REFERENCES

ADIKO S-B & MINGASOV RR. 2020. Crude Distillation Unit (CDU), Analytical Chemistry - Advancement, Perspectives and Applications, Abhay Nanda Srivastva, IntechOpen, 248 p. DOI: 10.5772/intechopen.90394. Available in <https://www.intechopen.com/chapters/72948>.

AUFLEM IH, KALLEVIK H, WESTVIK A & SJÖBLUM J. 2001. Influence of pressure and solvency on the separation of water-in-crude-oil emulsions from the North Sea. *J Petrol Sci Eng* 31: 1-12.

BAILEY NJL & KROUSE HR. 1973. Alteration of Crude Oil by Waters and Bacteria--Evidence from Geochemical and Isotope Studies. *AAPG Bull* 57: 1276-1290.

BONILLA JV & ENGEL MH. 1988. Chemical alteration of crude oils during simulated migration through quartz and clay minerals. *Org Geochem* 13: 503-512.

CHANG X, WANG G, GUO H, CUI J & WANG T. 2016. A case study of crude oil alteration in a clastic reservoir by waterflooding. *J Pet Sci Eng* 146: 380-391.

CHANG X, WANG Y, XU Y, CUI J & WANG T. 2018. On the changes of polycyclic aromatic compounds in waterflooded oil and their implications for geochemical interpretation. *Org Geochem* 120: 56-74.

CORILLO YE, VAZ BG, SIMAS RC, NASCIMENTO HDL, KLITZKE CF, PEREIRA RCL, BASTOS WL, SANTOS NETO EV, RODGERS RP & EBERLIN MN. 2010. Petroleomics by EASI(±) FT-ICR MS. *Anal Chem* 82: 3990-3996.

CUI J, ZHU R & HU J. 2014. Identification and geochemical significance of polarized macromolecular compounds in lacustrine and marine oils. *Chin J Geochem* 33: 431-438.

DE ARAUJO LLGC, SODRÉ LGP, BRASIL LR, DOMINGOS DF, DE OLIVEIRA VM & DA CRUZ GF. 2019. Microbial enhanced oil recovery using a biosurfactant produced by *Bacillus safensis* isolated from mangrove microbiota - Part I biosurfactant characterization and oil displacement test. *J Pet Sci Eng* 180: 950-957.

DE HEMPTINNE JC, PEUMERY R, RUFFIER-MERAY V, MORACCHINI G, NAIGLIN J, CARPENTIER B, OUDIN JL & CONNAN J. 2001. Compositional changes resulting from the water-washing of a petroleum fluid. *J Pet Sci Eng* 29: 39-51.

DOMINGOS DF, DE FARIA AF, GALAVERNA RS, EBERLIN MN, GREENFIELD P, ZUCCHI TD, MELO IS, TRAN-DINH N, MIDGLEY D & DE OLIVEIRA VM. 2015. Genomic and chemical insights into biosurfactant production by the mangrove-derived strain *Bacillus safensis* CCMA-560. *Appl Microbiol Biotechnol* 99: 3155-3167.

GÜRGEY K. 1998. Geochemical effects of asphaltene separation procedures: changes in sterane, terpane, and methylalkane distributions in maltenes and asphaltene co-precipitates. *Org Geochem* 29: 1139-1147.

HAN Y, POETZ S, MAHLSTEDT N, KARGER C & HORSFIELD B. 2018a. Fractionation and origin of NyOx and Ox compounds in the Barnett Shale sequence of the Marathon 1 Mesquite well, Texas. *Mar and Petrol Geology* 97: 517-524.

HEAD IM, LARTER SR, GRAY ND, SHERRY A, ADAMS JJ, AITKEN CM, JONES DM, ROWAN AK, HUANG H & ROLING WFM. 2010. Hydrocarbon degradation in petroleum reservoir. *Handbook of Hydrocarbon and Lipid Microbiology*, Springer-Verlag: Berlin.

HECKMANN JR, LANDAU L, GONÇALVES FTT, PEREIRA R & AZEVEDO DA. 2011. Avaliação geoquímica de óleos brasileiros com

- ênfase nos hidrocarbonetos aromáticos. *Quim Nova* 34: 1328-1333.
- HUGHEY CA, RODGERS RP, MARSHALL AG, QIAN K & ROBBINS WK. 2002. Identification of acidic NSO compounds in crude oils of different geochemical origins by negative ion electrospray Fourier transform ion cyclotron resonance mass spectrometry. *Org Geochem* 33: 743-759.
- KIM S, KRAMER RW & HATCHER PG. 2003. Graphical Method for Analysis of Ultrahigh-Resolution Broadband Mass Spectra of Natural Organic Matter, the Van Krevelen Diagram. *Anal Chem* 75: 5336-5344.
- KIM S, STANFORD LA, RODGERS RP, MARSHALL AG, WALTERS CC, QIAN K, WENGER LM & MANKIEWICZ P. 2005. Microbial alteration of the acidic and neutral polar NSO compounds revealed by Fourier transform ion cyclotron resonance mass spectrometry. *Org Geochem* 36: 1117-1134.
- KRYACHKO Y. 2018. Novel approaches to microbial enhancement of oil recovery. *J Biotechnol* 266: 118-123.
- KUO LC. 1994. An experimental study of crude oil alteration in reservoir rocks by water washing. *Org Geochem* 21: 465-479.
- LAFARGUE E & LE THIEZ P. 1996. Effect of water washing on light ends compositional heterogeneity. *Org Geochem* 24: 1141-1150.
- LARTER S, HUANG H, ADAMS J, BENNET B, JOKANOLA O, OLDENBURG T, JONES M, HEAD I, RIEDIGER C & FOWLER M. 2006. The controls on the composition of biodegraded oils in the deep subsurface: Part II—Geological controls on subsurface biodegradation fluxes and constraints on reservoir-fluid property prediction. *AAPG Bulletin* 90: 921-938.
- LARTER SR, APLIN AC, CORBETT PWM, EMENTON N, CHEN M & TAYLOR P. 1997. Reservoir geochemistry: A link between reservoir geology and engineering. *SPE Res Eng* 12: 12-17.
- LEITENMÜLLER V & RUPPRECHT BJ. 2019. A multidisciplinary approach for chemical EOR screening: Understanding alkali-oil interaction by the use of petroleum geochemistry. *J Petrol Sc Eng* 180: 967-981.
- LI H & ZHANG M. 2010. Geochemical characteristics of oils among real cores in displacement model. *Chin J Geochem* 29: 146-151.
- LIU P, LI M, JIANG Q, CAO T & SUN Y. 2015. Effect of secondary oil migration distance on composition of acidic NSO compounds in crude oils determined by negative-ion electrospray Fourier transform ion cyclotron resonance mass spectrometry. *Org Geochem* 78: 23-31.
- LIU Q, DONG M, ZHOU W, AYUB M, ZHANG YP & HUANG S. 2004. Improved oil recovery by adsorption-desorption in chemical flooding. *J Petrol Sc Eng* 43: 75-86.
- MAHLSTEDT N, HORSFIELD B, WILKES H & POETZ S. 2016. Tracing the Impact of Fluid Retention on Bulk Petroleum Properties Using Nitrogen-Containing Compounds. *Energy Fuel* 30: 6290-6305.
- MARSHALL AG & RODGERS RP. 2004. Petroleomics: The Next Grand Challenge for Chemical Analysis. *Acc Chem Res* 37: 53-59.
- MARSHALL AG & RODGERS RP. 2008. Petroleomics: Chemistry of the underworld. *Proc Natl Acad Sci USA* 105: 18090-18095.
- MARTINS LL, FRANKLIN GC, DE SOUZA ES & DA CRUZ GF. 2014. Pentacyclic Terpanes as Indicators of Compositional Heterogeneities in Biodegraded Oil Reservoir. *Quim Nova* 37: 1263-1268.
- MARTINS LL, PUDENZI MA, DA CRUZ GF, NASCIMENTO HDL & EBERLIN MN. 2017. Assessing Biodegradation of Brazilian Crude Oils via Characteristic Profiles of O₁ and O₂ Compound Classes: Petroleomics by Negative-Ion Mode Electrospray Ionization Fourier Transform Ion Cyclotron Resonance Mass Spectrometry. *Energy Fuel* 31: 6649-6657.
- MARTINS LL, SCHULZ HM, NOAH M, POETZ S, RIBEIRO HJPS & DA CRUZ GF. 2021. New paleoenvironmental proxies for the Irati black shales (Paraná Basin, Brazil) based on acidic NSO compounds revealed by ultra-high resolution mass spectrometry. *Org Geochem* 151: 104152.
- NIKOLOVA C & GUTIERREZ T. 2020. Use of Microorganisms in the Recovery of Oil from Recalcitrant Oil Reservoirs: Current State of Knowledge Technological Advances and Future Perspectives. *Front Microbiol* 10: 1-18.
- NIYONSABA E, MANHEIM JM, YERABOLU R & KENTTAMAA HI. 2019. Recent Advances in Petroleum Analysis by Mass Spectrometry. *Anal Chem* 91: 156-177.
- OLDENBURG TBP, BROWN M, BENNETT B & LARTER SR. 2014. The impact of thermal maturity level on the composition of crude oils, assessed using ultra-high resolution mass spectrometry. *Org Geochem* 75: 151-168.
- OLDENBURG TBP, BROWN M, HSIEH B & LARTER S. 2011. Fourier Transform Ion Cyclotron Resonance Mass Spectrometry – the analytical tool for heavy oil and bitumen characterization. CSP CSEG SWLS Convention.
- OLDENBURG TBP, JONES M, HUANG H, BENNETT B, SHAFIEE NS, HEAD I & LARTER SR. 2017. The controls on the composition of biodegraded oils in the deep subsurface – Part 4. Destruction and production of high molecular weight non-hydrocarbon species and destruction of

aromatic hydrocarbons during progressive in-reservoir biodegradation. *Org Geochem* 114: 57-80.

PEREIRA RCL ET AL. 2013. Precision in Petroleomics via Ultrahigh Resolution Electrospray Ionization Fourier Transform Ion Cyclotron Resonance Mass Spectrometry. *Energy Fuel* 27: 7208-7216.

PETERS KE & MOLDOWAN JM. 1991. Effects of source, thermal maturity, and biodegradation on the distribution and isomerization of homohopanes in petroleum. *Org Geochem* 17: 47-61.

PETERS KE, WALTERS CC & MOLDOWAN JM. 2005. Biomarkers and Isotopes in Petroleum Systems and Earth History, 2nd ed., Cambridge: Cambridge University Press. The Biomarker Guide: II.

PINTO FE, SILVA CFPM, TOSE LV, FIGUEIREDO MAG, SOUZA WC, VAZ BG & ROMÃO W. 2017. Evaluation of Adsorbent Materials for the Removal of Nitrogen Compounds in Vacuum Gas Oil by ESI(±)FT-ICR MS. *Energy Fuel* 31: 3454-3464.

POETZ S, HORSFIELD B & WILKES H. 2014. Maturity-driven generation and transformation of acidic compounds in the organic-rich Posidonia shale as revealed by electrospray ionization Fourier transform ion cyclotron resonance mass spectrometry. *Energy Fuel* 28: 4877-4888.

PRICE LC. 1976. Aqueous solubility of petroleum as applied to its origin and primary migration. *AAPG Bull* 60: 213-244.

QIAN K, RODGERS RP, HENDRICKSON CL, EMMETT MR & MARSHALL AG. 2001. Reading chemical fine print: Resolution and identification of 3000 nitrogen-containing aromatic compounds from a single electrospray ionization Fourier transform ion cyclotron resonance mass spectrum of heavy petroleum crude oil. *Energy Fuel* 15: 492-498.

ROCHA YS, PEREIRA RCL & MENDONÇA FILHO JG. 2017. Negative electrospray Fourier transform ion cyclotron resonance mass spectrometry determination of the effects on the distribution of acids and nitrogen containing compounds in the simulated thermal evolution of a Type-I source rock. *Org Geochem* 115: 32-45.

ROCHA YS, PEREIRA RCL & MENDONÇA FILHO JG. 2018. Geochemical characterization of lacustrine and marine oils from off-shore Brazilian sedimentary basins using negative-ion electrospray Fourier transform ion cyclotron resonance mass spectrometry (ESI FTICR-MS). *Org Geochem* 124: 29-45.

ROCHA YS, PEREIRA RCL & MENDONÇA FILHO JG. 2019. Geochemical assessment of oils from the Mero Field, Santos Basin, Brazil. *Org Geochem* 130: 1-3.

RODGERS RP, SCHAUB TM & MARSHALL AG. 2005. Petroleomics: MS returns to its roots. *Anal Chem* 77: 20A-27A.

SAFDEL M, ANBAZ MA, DARYASAFAR A & JAMIALAHMADI M. 2017. Microbial enhanced oil recovery, a critical review on worldwide implemented field trials in different countries. *Renew. Sustain. Energy Fuel* 74: 159-172.

SHE H, KONG D, LI Y, HU Z & GUO H. 2019. Recent Advance of Microbial Enhanced Oil Recovery (MEOR) in China. *Geofluids*: 1-16.

SHI Q, ZHAO S, XU Z, CHUNG KH, ZHANG Y & XU C. 2010. Distribution of acids and neutral nitrogen compounds in a Chinese crude oil and its fractions: characterized by negative-ion electrospray ionization Fourier transform ion cyclotron resonance mass spectrometry. *Energy Fuel* 24: 4005-4011.

SOLOMONS TWG, FRYHLE CB & SNYDER SA. 2016. Organic Chemistry, J Wiley & Sons Inc., 1200 p., 12th ed, U.S.

SOUZA LM, TOSE LV, CARDOSO FMR, FLEMING FP, PINTO FE, KUSTER RM, FILGUEIRAS PR, VAZ BG & ROMÃO W. 2018. Evaluating the effect of ion source gas (N₂, He, and synthetic air) on the ionization of hydrocarbon, condensed aromatic standards, and paraffin fractions by APCI(+)-FT-ICR MS. *Fuel* 225: 632-645.

SPEIGHT JG. 2006. Chemistry and Technology of Petroleum, 4th ed. Hoboken: Taylor and Francis, 984 p.

SULEIMANOV B, SALMANOV A & ZEYNALOV E. 2020. Oil recovery stages and methods. Primer on Enhanced Oil Recovery, Gulf Professional Publishing, Oxford.

TERRA LA, FILGUEIRAS PR, TOSE LV, ROMÃO W, DE CASTRO EVR, DE OLIVEIRA LMSL, DIAS JCM, VAZ BG & POPPI RJ. 2015. Laser desorption ionization FT-ICR mass spectrometry and CARSPLS for predicting basic nitrogen and aromatics contents in crude oils. *Fuel* 160: 274-281.

TRINDADE LAF & BRASSELL SC. 1992. Geochemical assessment of petroleum migration phenomena on a regional scale: case studies from Brazilian marginal basins. *Org Geochem* 19: 13-27.

VAZ BG, SILVA RC, KLITZKE CF, SIMAS RC, NASCIMENTO HDL, PEREIRA RCL, GARCIA DF, EBERLIN MN & AZEVEDO DA. 2013. Assessing biodegradation in the Llanos Orientales crude oils by electrospray ionization ultrahigh resolution and accuracy Fourier transform mass spectrometry and chemometric analysis. *Energy Fuel* 27: 1277-1284.

WAN Z, LI S, PANG X, DONG Y, WANG Z, CHEN X, MENG X & SHI Q. 2017. Characteristics and geochemical significance of heteroatom compounds in terrestrial oils by negative-ion electrospray Fourier transform ion cyclotron resonance mass spectrometry. *Org Geochem* 111: 34-55.

XU Y, WANG T, CHEN N, YANG C & WANG Q. 2012. DBT parameters and dynamic monitoring during reservoir development,

and distribution region prediction of remaining oil: a case study on the Sha-33 oil reservoir in the Liubei region, Nanpu sag. *Sci China Earth Sci* 55: 2018-2025.

ZHANG Y, SHI Q, LIA, CHUNG KH, ZHAOS & XU C. 2011. Partitioning of Crude Oil Acidic Compounds into Subfractions by Extrography and Identification of Isoprenoidyl Phenols and Tocopherols. *Energy Fuel* 25: 5083-5089.

ZHU Y & LEI M. 2015. Effects of Crude Oil Components on the Interfacial Tension Between Oil and Surfactant Solutions. *SPE Asia Pacific Enhanced Oil Recovery Conference*.

ZHU Y, WENG H, CHEN Z & CHEN Q. 2003. Compositional modification of crude oil during oil recovery. *J Pet Sci Eng* 38: 1-11.

ZIEGS V, PÖTZ S, HORSFIELD B, RINNA J, HARTWIG A & SKEIE JE. 2018. Deeper Insights into Oxygen-Containing Compounds of the Mandal Formation. *Central Graben, Norway*. *Energy Fuel* 32: 12030-12048.

SUPPLEMENTARY MATERIAL

Appendix A: Tables SI-SIII. Figures S1-S2.

How to cite

SODRÉ LGP, MARTINS LL, DE ARAUJO LLGC, FRANCO DMM, VAZ BG, ROMÃO W, MERZEL VM & DA CRUZ GF. 2022. Implications of microbial enhanced oil recovery and waterflooding for geochemical interpretation of recovered oils. *An Acad Bras Cienc* 94: e20211433. DOI 10.1590/0001-3765202220211433.

*Manuscript received on October 25, 2021;
accepted for publication on February 1, 2022*

LUCIANA G.P. SODRÉ¹

<https://orcid.org/0000-0002-6307-6307>

LAERCIO L. MARTINS¹

<https://orcid.org/0000-0001-6216-990X>

LORRAINE LOUISE G.C. DE ARAUJO^{1,2}

<https://orcid.org/0000-0003-0661-3759>

DANIELLE M.M. FRANCO³

<https://orcid.org/0000-0002-3691-4328>

BONIEK G. VAZ³

<https://orcid.org/0000-0003-1197-4284>

WANDERSON ROMÃO⁴

<https://orcid.org/0000-0002-2254-6683>

VALÉRIA M. MERZEL⁵

<https://orcid.org/0000-0001-8817-4758>

GEORGIANA F. DA CRUZ¹

<https://orcid.org/0000-0003-2116-2837>

¹Universidade Estadual do Norte Fluminense Darcy Ribeiro (UENF), Laboratório de Engenharia e Exploração de Petróleo (LENEP), Rodovia Amaral Peixoto, Km 163, Avenida Brennand, Imboassica, 27925-535 Macaé, RJ, Brazil

²Universidade Federal do Rio de Janeiro (UFRJ), Instituto de Química, Avenida Athos da Silveira Ramos, 149, Ilha do Fundão, 21941-909 Rio de Janeiro, RJ, Brazil

³Universidade Federal de Goiás (UFG), Instituto de Química, Avenida Esperança, Chácaras de Recreio Samambaia, 74690-900 Goiânia, GO, Brazil

⁴Universidade Federal do Espírito Santo (UFES), Avenida Fernando Ferrari, 514, Goiabeiras, 29075-910 Vitória, ES, Brazil

⁵Universidade Estadual de Campinas (UNICAMP), Centro Pluridisciplinar de Pesquisas Químicas, Biológicas e Agrícolas (CPQBA), Avenida Alexandre Cazellato, 999, Paulínia/Betel, 13148-218 São Paulo, SP, Brazil

Correspondence to: **Georgiana Feitosa da Cruz**

E-mail: georgiana@lenep.uenf.br

Author contributions

Sodré LGP: experimental work, conceptualization, writing and editing. Martins LL: treatment concerning the results from FT-ICR MS. De Araujo LLGC: core flooding experiment and treatment concerning the results from core flooding experiment. Franco DMM: made oils analyses in 7T Solarix 2xR ESI(-) FT-ICR mass spectrometer (Bruker Daltonics, Bremen, Germany). Vaz BG: suport and discussion from FT-ICR MS analysis obtained in a 7T Solarix 2xR ESI(-) FT-ICR mass spectrometer. Romão W: suport and discussion from FT-ICR MS analysis obtained in a Solarix 9.4T ESI(+) FT-ICR mass spectrometer. Merzel VM: isolated and supplied the biosurfactant for the core flooding experimente. Da Cruz GF: conceptualization, writing, discussion, review and supervision.

